



Study of seismic site effects and soil-structure resonance of Bhaktapur District, Nepal using microtremors

Chandra Kiran Kawan · Amit Prajapati ·
Dinesh Sakhakarmi

Received: 7 September 2023 / Accepted: 13 March 2024 / Published online: 2 April 2024
© The Author(s), under exclusive licence to Springer Nature B.V. 2024

Abstract Bhaktapur city, one of the historical cities of Nepal, is among the old settlements within Kathmandu Valley that were frequently devastated during major earthquakes. Historical evidence clearly states the high seismic vulnerability of Bhaktapur. So, this study characterizes the free field of the Bhaktapur district in terms of periods. For this, the horizontal to vertical (H/V) technique was used to determine the predominant period of the study area, measuring microtremor data at 200 m×200 m spacing in the core city area, whereas 400 m×400 m spacing of measurement was done at the outskirts of the city with rare settlement. The spatial distribution map of the predominant period is prepared with the period obtained from 609 measuring points. The map shows that the predominant period ranges from 0.1 to 4 s and then categorized into four different zones—A

(0.10–0.6 s), B (0.6–1.0 s), C (1.0–1.7 s), and D (1.7–4.0 s). The central parts of the study areas are spotted with longer periods (1.7–4.0 s), where the density of the dweller is high. The structural period of 28 reinforced concrete buildings was also determined to understand the level of danger of the buildings due to soil-structure resonance. The predominant period of the buildings ranges from 0.12 to 0.42 s. The possibility of soil structure resonance condition is higher for six buildings, medium for two buildings, and low for the rest of the buildings. The results can be applied to urban planning, seismic hazard mitigation, conservation, and restoration of heritage monuments.

Keywords Microtremor · H/V spectral ratio · Floor spectral ratio · Predominant period · Seismic zonation · Soil-structure resonance

C. K. Kawan (✉)
Department of Civil Engineering, Khwopa College
of Engineering, Tribhuvan University, Libali, Nepal
e-mail: kawan.chandra1@gmail.com

A. Prajapati
State Key Laboratory of Disaster Reduction in Civil
Engineering, Tongji University, Shanghai 200092, China
e-mail: amit@tongji.edu.cn

D. Sakhakarmi
M.E in Earthquake Engineering, Department
of Earthquake Engineering, Khwopa Engineering College,
Purbanchal University, Libali, Nepal
e-mail: sakha.dinesh1996@gmail.com

1 Introduction

Bhaktapur, one of the oldest cities of the Kathmandu Valley, Nepal, is rich in tangible and intangible heritage. The central city of Bhaktapur is renowned for its traditional cultures and ancient monuments, which were built back in Nepal's medieval era. In every major earthquake, the Bhaktapur district experiences heavy destruction than other districts of the Valley (Tallett-Williams et al. 2016; Kawan et al. 2022a). The latest seismic event was observed as the Gorkha earthquake 2015, 7.8 Mw struck at Barpak, Gorkha

around 90 km northwest. The damages were reported by Gilder et al. (2020) and McGowan et al. (2017). Around 28,508 buildings collapsed and 9054 buildings were partially damaged by this seismic event (MoHA 2015). Similarly, the destruction in Bhaktapur was also observed higher in the 1988 Udayapur earthquake and the 1934 Nepal-Bihar earthquake (Pandey and Molnar 1988; Kawan et al. 2022a). The regular destruction during major earthquakes underlined the importance of ground seismic study in the eastern part of the Valley, Bhaktapur district.

In the prehistoric era, Kathmandu Valley used to be a lake with a bowl-like shape, filled with unconsolidated quaternary sediment (Bijukchhen 2018; Kawan et al. 2022a). Later, it was developed as a historic city. The spatial variation of these fluvial and lacustrine deposits in the basin varies accordingly. Moribayashi and Maruo (1980) measured the deepest sediment thickness of 650 m using the gravity technique in the Northwest of Singha Durbar, Kathmandu. These unconsolidated settlements with varying depths exhibit high seismic waveform during seismic events depending upon the impedance contrast of different layers of deposit (Bonney-Claudet et al. 2009; Bijukchhen 2018). The propagated seismic wave properties (frequency content, duration, amplitude) produce a peculiar response at the ground surface. Previous studies (Pandey 2000; Paudyal et al. 2012b, a; Kawan et al. 2022a) have quantified the various local soil amplification factors at various places in Kathmandu Valley due to the deposit of unconsolidated soil sediment. These studies have suggested the amplification factor ranging from 1.8 to 8.5 for different parts of the Kathmandu Valley. Gorkha Earthquake (2015), Nepal, exposed the vulnerability of the existing construction, as evidenced by the site amplification caused by the soft ground in the Kathmandu Valley. The seismic amplification characteristic study of the Kathmandu Valley is compared with the Mexico City 1985 Michoacan earthquake (Towhata 2007; Takai et al. 2016; Bijukchhen 2018; Parajuli et al. 2021) as damages caused due to seismic amplification are similar in both cities. Within the same area, local site amplification can cause noticeable variations in structural damage. Another aspect is the resonance of the fundamental frequencies between the building and the soil sediment, which increases the vulnerability of the structure. The seismic ground motion will resonate with the building if the building's natural

frequency is close to that of the soil (Gosar 2010, 2012). The resonating frequency of the building and the soil sediments on which the building is constructed are the most significant components in the prediction of earthquake building damage distribution (Stanko et al. 2017). So, the destruction scenario during the strong ground motions can be predicted by quantifying these two basic ground motion parameters- seismic amplification factor and resonance frequency between the soil and building.

The HVSr (horizontal to vertical spectral ratio) method was introduced firstly by Nogoshi and Igarashi (1970, 1971) and was later popularized by Nakamura (1989). This method is a non-destructive technique and the easiest and cheapest way to understand the ground vibration characteristics. Due to its simplicity, many researchers have widely adopted for the determination of the fundamental frequency (Field and Jacob 1993; Ohmachi et al. 1994; Gallipoli et al. 2004b) and seismic amplification (Lermo and Chávez-García, 1994; Konno and Ohmachi 1998) of the ground surface. Generally, in densely populated areas, the HVSr tool is popular since other methods would be too invasive, too expensive, or otherwise inappropriate given the presence of civilization (Nogoshi 1971; Nakamura 1989; Mucciarelli and Gallipoli 2001; Gosar 2010). In this method, the ambient noise is measured in three directions—one vertical direction and two horizontal directions. These measured noises are processed to obtain the Fourier spectra using the fast Fourier transform (FFT) and ultimately obtain the ratio of horizontal to vertical spectrum ratio. The H/V analysis tools represent the site characterization in terms of shear velocity, the thickness of soil units, resonating frequency, and the depth of engineering bedrock (García-Fernández and Jiménez 2012; Moisidi et al. 2015). It has been successfully deployed in Kathmandu Valley to understand the spatial distribution of fundamental frequencies and seismic amplitude of the ground surface of the Kathmandu Valley. Kawan et al. (2022a) conducted a site response analysis of Bhaktapur City and the result obtained from the numerical analysis was validated using the H/V spectral ratio. It showed that the spatial distribution of fundamental frequencies obtained from numerical analysis and the H/V spectral ratio were closely matched. Yamada et al. (2016) conducted the microtremor measurement in the Kathmandu Valley and Sindhupalchok district to understand the intensity of damages due to the 2015 Gorkha Earthquake. Pandey (2000) carried out the microtremor

measurement in the 60 sites of the Kathmandu Valley to understand the site amplification and found the peak amplification in the range of 12–15. Bhandary et al. (2014) conducted microtremor measurements in 172 points of Kathmandu Valley to prepare a period-dominant shaking map and the geo-database of the Kathmandu Valley. Paudyal et al. (2012b, a) determined the spatial distribution of the fundamental frequency of soil deposits in Kathmandu Valley using the HVSR method and showed that the fundamental frequency of soil deposits ranged from 0.49 to 8.9 Hz.

The microtremor measurement is also extensively used in buildings to assess the dynamic structural properties like the fundamental frequency, damping ratio, modal vibration, and even in the study of the soil-structure interaction (Irie and Nakamura 2000; Mucciarelli et al. 2001; Gallipoli et al. 2004a). This technique also has the advantage of being viable without the need for simultaneous measurements while still producing accurate representations of the linear elastic behavior of the structures in the frequency domain (Lermo and Chivez-Garcfa 1993). Castro et al. (2000) proved the reliability of this method for the identification of the fundamental frequencies of the earthen and concrete dams. By analyzing the soil sediment of the ancient city's ruins in Aptaera (Greece) using the HVSR method, Moisiidi et al. (2004) were able to determine the cause of the primary structural damage mechanism. The soil-structure resonance condition and building damage assessment were also studied using microtremors for the Umbria-Marche earthquake (Mucciarelli and Monachesi 1998; Natale and Nunziata 2004), Thessaloniki earthquake (Panou et al. 2005), Molise earthquake (Gallipoli et al. 2004b), the Ilirska Bistrica area (Gosar and Martinec 2008), and the Ljubljana basin (Gosar et al. 2010). Nakamura et al. (2000) and Nakamura et al. (1999) also extend the HVSR method in measuring the vibratory frequencies of cultural heritage structures such as the Roman Colosseum and the Leaning Tower of Pisa. Parajuli et al. (2021) deployed the HVSR method to determine the fundamental frequency and damping ratio of the two-story old heritage building. Gosar et al. (2010) utilized microtremors to assess the site effects and soil-structure resonance in the Kobarid basin (Slovenia). The study prepared the iso-frequency map of the sediments and compared free-field sediment frequencies derived from the iso-frequency map with the measured fundamental

frequencies of 19 buildings. The study concluded by stating that the danger of soil-structure resonance is evident in the Kobarid areas, especially in the transition zone. Stanko et al. (2017) examined the potential danger of soil structure in Varazdin City (North Croatia) by comparing microtremor measurements conducted in buildings and nearby free-field locations using standard spectral ratio and floor spectral ratio. Their results show that taller buildings up to 11 floors have a higher potential for soil-structure resonance. Giocoli et al. (2019) applied the HVSR technique to understand the foundation geometry and resonance frequencies between the structure-site of the Orvieto Cathedral of Umbria in central Italy. Kawan et al. (2022b) used the HVSR method in the dynamic characterization of the exposed foundation of the multi-tiered temples and the soil deposit of the old heritage sites of Kathmandu Valley and present the possibility of resonance between the soil and multi-tiered temples. Gallipoli et al. (2020) evaluated the effect of the soil-building resonance in the urban area of Matera, Italy and argued that about 21% of buildings show a higher probability of soil-structure resonance effect and 36% of buildings are characterized by a medium resonance level. Bhandary et al. (2021) studied the resonance effect on the vibration of tall buildings built in the Kathmandu Valley during the 2015 Gorkha earthquake using the HVSR method. Gangone et al. (2023) conducted a microtremor test on the urban soils of Villa d'Agri town and compared the obtained sediment frequency with the frequency of the building to understand the soil-structure resonance condition. This study reveals that the probability of being affected by double resonance is very high for 0.3% of buildings, high for about 16% of buildings, moderate for 23%, and null for the remaining 60% of buildings.

In the urban built areas, the microtremor measurement can be contaminated by the vibration of the existing buildings. Different studies have shown that the influence of a building's vibration is observed in HVSR functions while determining the free-field site response. At the Hera Lacinia Column site in Italy, Mucciarelli et al. (1996) measured the microtremor H/V spectral ratio and identified the column's first vibration mode at approximately 0.5 Hz. At this frequency, a peak was also observed in the free-field measurement near column, with amplitude decreasing as distance

increased. The outcome also showed that the peak lost significance at a distance approximately equal to the column's height. Tenta et al. (2001) also observed that the amplitude functions of spectral ratio deduced from a reference structure suggested the possible contamination of the building's vibration in the free-field measurement. Gallipoli et al. (2004a) conducted a microtremor test on the tall water tower structure and at four spaced sites (0 m, 12 m, 30 m, 100 m) from the tall water tower in Macerata, Italy. This study also concluded that the measured frequencies of the sites contain the vibration frequency of the water tower, whose peak amplitude decreases as distance increases. Laurenzano et al. (2010) conducted a study on two adjacent buildings located in Bonefro that were affected by the 2002 Molise earthquake (Italy) and stated that the effect of building vibration on the free-field motion was about 30–40% on spectral values up to the distance of approximately twice the height of the structure. Many other experimental studies (Kanamori et al. 1991; Gueguen et al. 2000; Gallipoli et al. 2006; Bindi et al. 2015; Petrovic and Parolai 2016) have also shown that the presence of buildings in densely urban areas modifies the ground motions compared to free-field conditions. The purpose of this study is to identify the dominant period of the free-field, prepare a seismic zonation map, and comprehend the soil-structure resonance condition. For this purpose, microtremor measurement was conducted in the free-field and buildings. The microtremor measurement was conducted in 200 m × 200 m grid spacing in the core city areas of the district, and on the outskirts, where the settlement is rare, measurement was done in 400 m × 400 m grid spacing. A total of 609 microtremor data points across the Bhaktapur district were collected. The collected data were then analyzed using the HVSr method to obtain the predominant period. The spatial distribution map of the predominant period was also prepared. Furthermore, the microtremor measurements were conducted in 28 buildings located in the study area and fundamental periods were obtained using the floor spectral ratio (FSR). The buildings' periods were overlaid in the sediment period map to understand the condition of soil-structure resonance in the study areas.

2 Geology of study area

Bhaktapur district, one of the smallest districts of Nepal, lies in the eastern part of the Kathmandu Valley covering an area of 119 km². This district is geopolitically divided into four municipalities—Bhaktapur, Changunarayan, Madhyapur Thimi, and Suryabinayak, as shown in Fig. 1. Bhaktapur district lies between 27° 37' to 27° 45' N latitude and 85° 17' to 85° 31' E longitudes, with a mean elevation of 1401 m above sea level. The population density of Bhaktapur district is 3631 per sq. km.

The Precambrian to Devonian rocks that make up the district's basement are highly faulted, folded, and fractured igneous and meta-sedimentary rocks (Sakai 2001). These rocks are then covered by a 550–600-m-thick Quaternary fluvial-lacustrine deposit (Piya 2004). According to Shrestha et al. (1999), the Bhaktapur district is situated in a weak geological structure with numerous fault lines, low-bearing capacity, and loose soil structure. The soil columns of the Bhaktapur district indicate that the topmost layer, ranging up to 15 m depth, is a deposit of silty clay with low to medium plasticity and is followed by black clay with a depth ranging from 15 to 130 m, underlaid by coarse sediments like coarse sand and gravel with the depth ranging from 130 to 290 m, and ultimately followed by bedrock (Kawan et al. 2019, 2022a). The sediment deposit of the Bhaktapur district is relatively finer, indicating the deposition might have occurred from suspension settling and the thin, parallel lamination of alternating silt and silty clay over sand beds (Paudyal 2015). The geological map prepared by the Department of Mines and Geology (DMG 1998), as shown in Fig. 1, shows that the study area is formed from the Kalimati Formation, Kulekhani Formation, Tistung Formation, and Gokarna Formation. The Kalimati Formation has recent floodplain deposits of the Hanumante River in the northern-west part and the Tistung Formation is in the southern-east part of the study area. Black clay, gray to dark silty clay with fine sand substrate, organic clay, and peat layers make up the Kalimati Formation (Sakai 2001; Paudel and Sakai 2008). The Gokarna Formation soil is characterized by light to brownish-gray, finely laminated, and poorly graded silty sand; loose to slightly compact with moderate to high bearing capacity (Sakai 2001; Rajaure 2021). The Tistung Formation is made up of slate, quartzite, and phyllite, whereas the Kulekhani Formation is

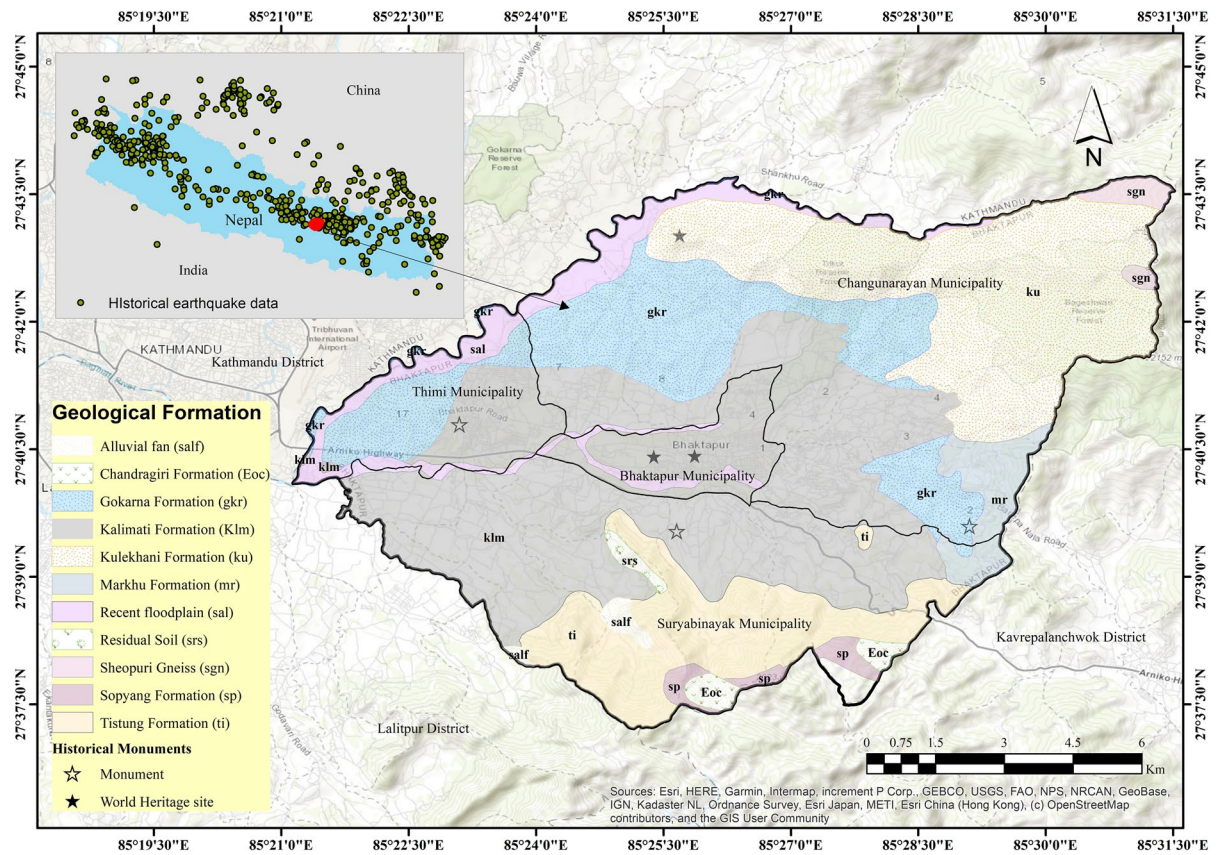


Fig. 1 Engineering geological features of Bhaktapur district. Top left inset map shows the seismic activities that occurred in Nepal along with the location of the study area

a well-bedded alternation of fine-grained biotic schist and micaceous quartzites (Thapa 1985; Sakai 2001). Most of the urban settlements of Kathmandu Valley are dwelled over the Gokarna Formation and Kalimati Formation (Shrestha et al. 2004). The dominant soil over the Kalimati and Gokarna Formations is Kalimati clay/black clay, which is characterized as soft soil and is the main possible cause of seismic amplification at the free-field of the study area.

3 Methodology

In the present study, microtremor measurements were performed using a portable velocity meter, the Geophone HG-6 manufactured by HGS (India) Limited with technology transfer from Sensor Netherland BV, operating at a frequency 4.5 Hz. The Thermo-Dolfrang data acquisition software was utilized for

measuring microtremors. This microtremor instrument takes the three-point measurements, including two horizontal directions (east–west direction and north–south direction) and one vertical direction (up–down direction). The data were measured at 100 Hz for 15 min at night to avoid unwanted artificial noise. The open-source application, GEOPSY software, was employed to process and analyzed the recorded velocity–time history data. Anti-triggering was performed in GEOPSY software to eliminate the transient noises present in the raw signal. For this, the short-time average (STA) and long-time average (LTA) values were set to 1 and 25 s, respectively. The minimum ratio of STA to LTA was set to 0.2 and the maximum ratio of STA to LTA was set to 2 (SESAME 2004). To illustrate, the velocity–time history data of one particular measured site is shown in Fig. 2, including the transient noise. About 25–30 stationary windows, obtained after the removal of transient noise, were

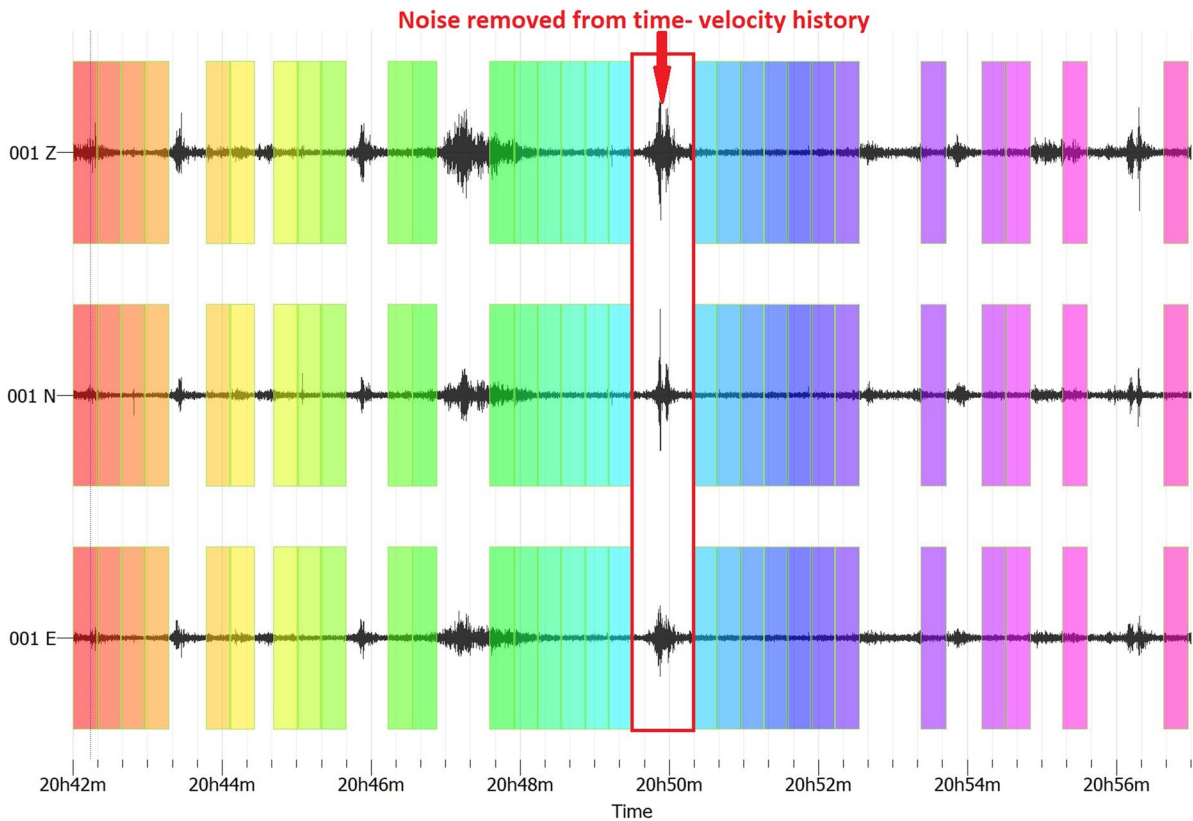


Fig. 2 Typical velocity time history graph of measured data showing the removal of noise in all three directions (vertical direction (Z), north-south direction(N), east-west direction (E))

used to obtain the Fourier amplitude spectra. The Fourier amplitude spectra were obtained using the fast Fourier transformation (FFT) for each window. The obtained Fourier amplitude spectra were then smoothed using the method proposed by Konno and Ohmachi (1998), with a smoothing constant of 40 tapers and a 5% cosine function. The square average approach was used to compute the average H/V spectral ratio for numbers of H/V spectral ratios obtained from each analyzed window of a particular measured point. From this average H/V spectral ratio, the fundamental frequency and the site amplification were obtained. The clear peak of the H/V spectral ratio represents the fundamental frequency of the free-field and structure (Gallipoli et al. 2004b; SESAME 2004; Gosar 2010; Paudyal et al. 2012b, a). The reliability of HVSR curves depends on several data acquisition and processing criteria that are adopted. The most important criteria concern with the data acquisition and extraction of continuous records of analysis

time windows for the evaluation of an HVSR function, which is dominated by the effects of buried geological structure (Koller et al. 2004; D'Alessandro et al. 2016). The data acquisition process needs special attention regarding recording parameters, recording duration, measurement spacing, in situ soil-sensor coupling, artificial soil-sensor coupling, sensor setting, nearby structures, weather conditions, and disturbances (SESAME 2004). The effect of transient seismic noise on HVSR analysis is still debated. The spikes and transients in microtremors are highly dependent on their sources and therefore cannot be used to estimate resonance frequencies of sites (Horike et al. 2001; Koller et al. 2004). On the other hand, some authors (Mucciarelli and Gallipoli 2004; Parolai and Galiana-Merino 2006; Parolai et al. 2009) suggest that spikes and transient noise windows should not be removed as they generally carry subsoil information. For the best estimate of mean HVSR curves, the elementary analysis windows in

continuous noise recordings are often chosen by visual inspection. A successive time window of the proper duration is used to calculate the HVSR curves. The process of selecting the best time frames to utilize in the computation of the site’s representative HVSR curve is frequently very challenging. This selection criterion yields results that are dependent on the operator’s subjective judgment, the dependability of which cannot be evaluated using quantitative measures (D’Alessandro et al. 2016). These highlight some of the uncertainties in experimental conditions, data acquisition, data processing, and extraction to obtain reliable HVSR curves and resonance frequencies of the sites. In this study, reliability and clarity criteria were also examined following SESAME (2004) standards to identify the clear HVSR peaks of each station.

The study area is divided into closely spaced grid sizes of 200×200 m in a GIS environment for microtremor measurement as shown in Fig. 3. This prepared map was then exported to Google Earth Pro to know the precise location of measurement stations. The microtremor measuring station was located in the field using a geographic positioning system (GPS), and reference sites such as roads, schools, and governmental buildings were used for exact location. The microtremor measurement was conducted two grid spacings: for densely inhabited areas like the core cities of Bhaktapur municipality, Surabinayak municipality, Madhyapur Thimi municipality, and Changunarayan municipality, the measurement was done with a grid spacing of 200×200 m, while on the outskirts of these municipalities, where the population density is low,

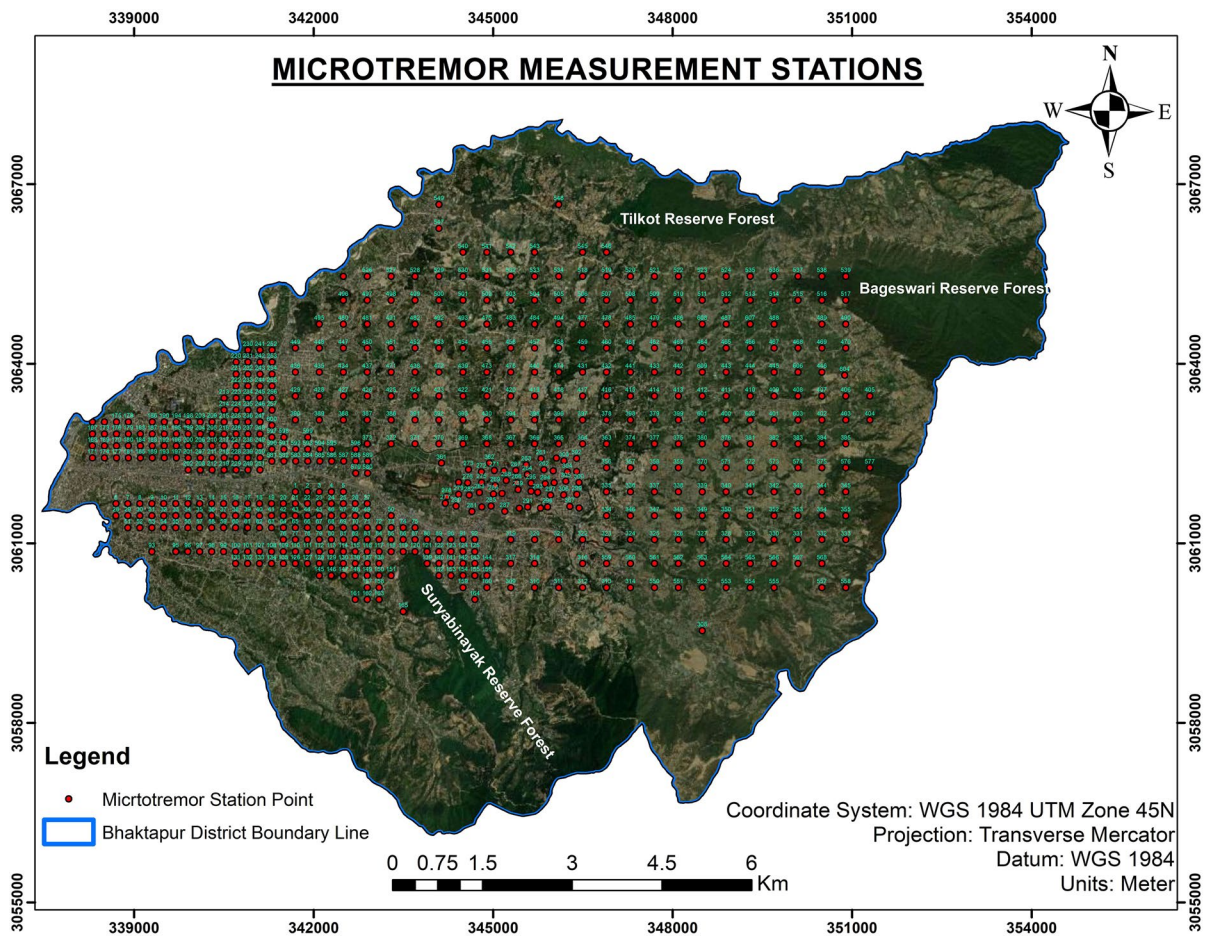


Fig. 3 Microtremor measurement stations in 200×200 m and 400×400 m grid spacing

the measurement was done in the grid spacing of 400×400 m as shown in Fig. 3. In case of densely inhabited areas, off-grid measurements were also carried out, as shown in Fig. 3. The locations were carefully chosen to avoid the influence of nearby structures, sources of monochromatic noise, and strong topographic features (such as edges of terraces). Additionally, measurements were not conducted on windy days, as the noise introduced by strong wind severely affects the reliability of HVSR analysis (SESAME 2004). In the old city, the free-field space between houses is also very limited. In such places, to eliminate the effect of buildings' presence in the free-field measurement, ground measurements were carried out at a distance at a distance equal to or greater than the height of the buildings, as much as possible. Many researchers (Mucciarelli et al. 1996; Tento et al. 2001; Gallipoli et al. 2004a, 2020) have pointed out that the effect of building vibration on soil is insignificant at a

distance approximately equal to the height of nearby structures. A total of 609 points were ascertained for measurement.

To understand the soil-structure resonance, the microtremor measurements were conducted in the buildings. The majority of structures in the studied areas are reinforced concrete buildings with infilled masonry walls, except in a few old settlements where load-bearing brick masonry structures are present. The buildings with 2–5 stories predominate in the study areas. Figure 4 shows the locations of the buildings considered for the microtremor measurements. A total of 28 single-standing isolated reinforced cement concrete (RCC) buildings were selected, the majority of which are residential and a few institutional. Noise data were recorded on two floors of each building- one set on the top floor and another set on the bottom floor. The microtremor device was placed near or at the center of mass of each building or close to the central column to

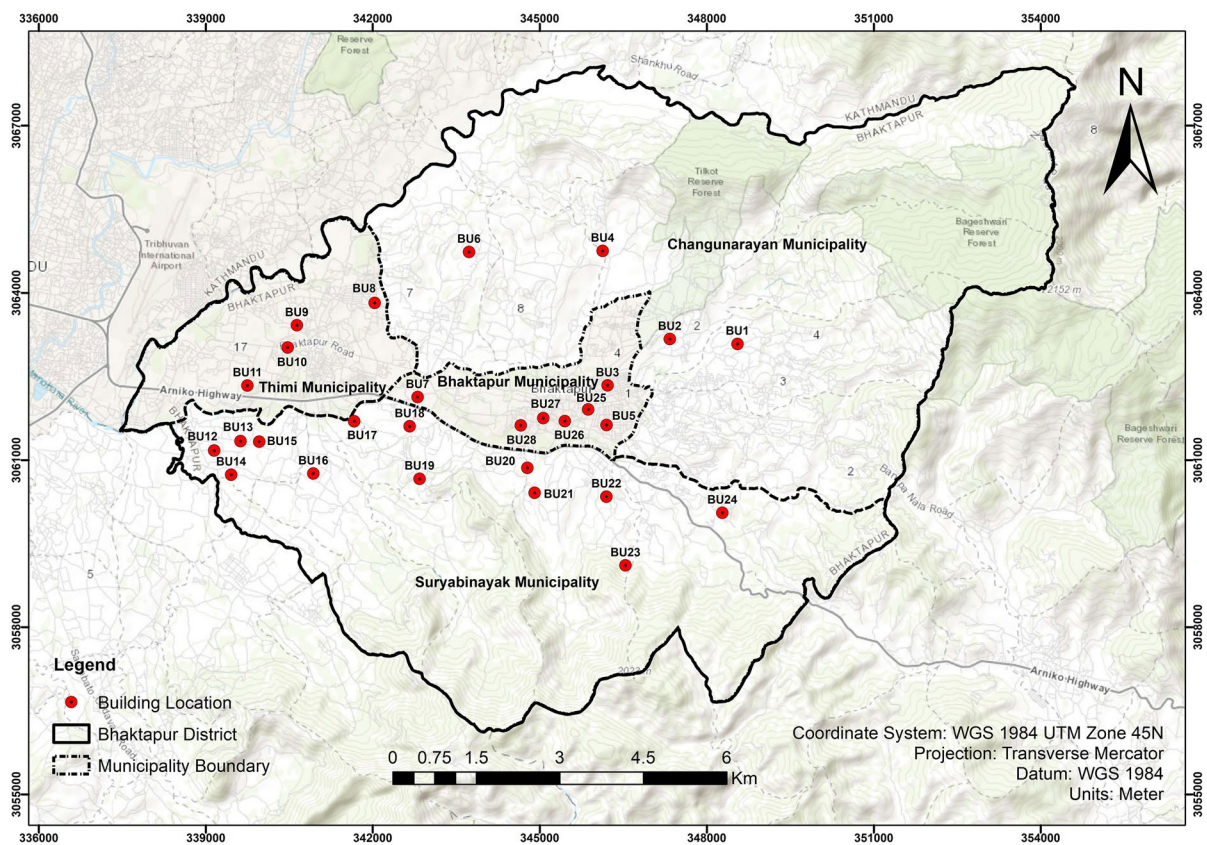


Fig. 4 Location of buildings considered during the study

minimize the impact of torsional frequency (Galipoli et al. 2004a; Parolai et al. 2005). The longitudinal and transverse directions of the building were set parallel to the two horizontal components of the microtremor as shown in Fig. 5a. A typical isolated RCC building considered for measurement is given in Fig. 5b, and the instrumental recording carried on the top and bottom floor of the building is shown in Fig. 5c. The measurement was conducted for 5 min on both the top and bottom floors of the building, in quiet times without any disturbances. A window length of 20 s was used for the analysis of the signals, along with a smoothing window (Konno and Ohmachi 1998) with a smoothing constant of 40 tapered with a 5% cosine function. Transients and erratic signals were eliminated using anti-triggering for each direction’s raw signal. The floor spectral ratio (FSR) was obtained by taking the ratio of horizontal components of the top floor and bottom floor for both longitudinal and transverse directions. From the computed FSR, the fundamental period of the buildings was determined.

4 Result and discussion

4.1 Free-field microtremor measurement

Some examples of the HVSR plots of the free-field station are displayed in Fig. 6. The HVSR curve of the majority of the stations fulfills the reliability and clarity criteria recommended by SESAME (2004) guidelines. The reliability check of the HVSR graph consists of three criteria which are related to the window length, the number of significant cycles, and the standard deviation of the peak H/V amplitude. The six criteria for the clarity check of the HVSR curve depend upon H/V amplitude, the standard deviation of frequency, and threshold values for the stability conditions. If all three criteria of reliability checks and five out of six criteria of clarity checks are fulfilled, the period corresponding to peak amplitude is considered to be the predominant period of the sediments. Low amplitude with flat HVSR peaks, multiple HVSR peaks, and significant levels of noise could all contribute to the failure of

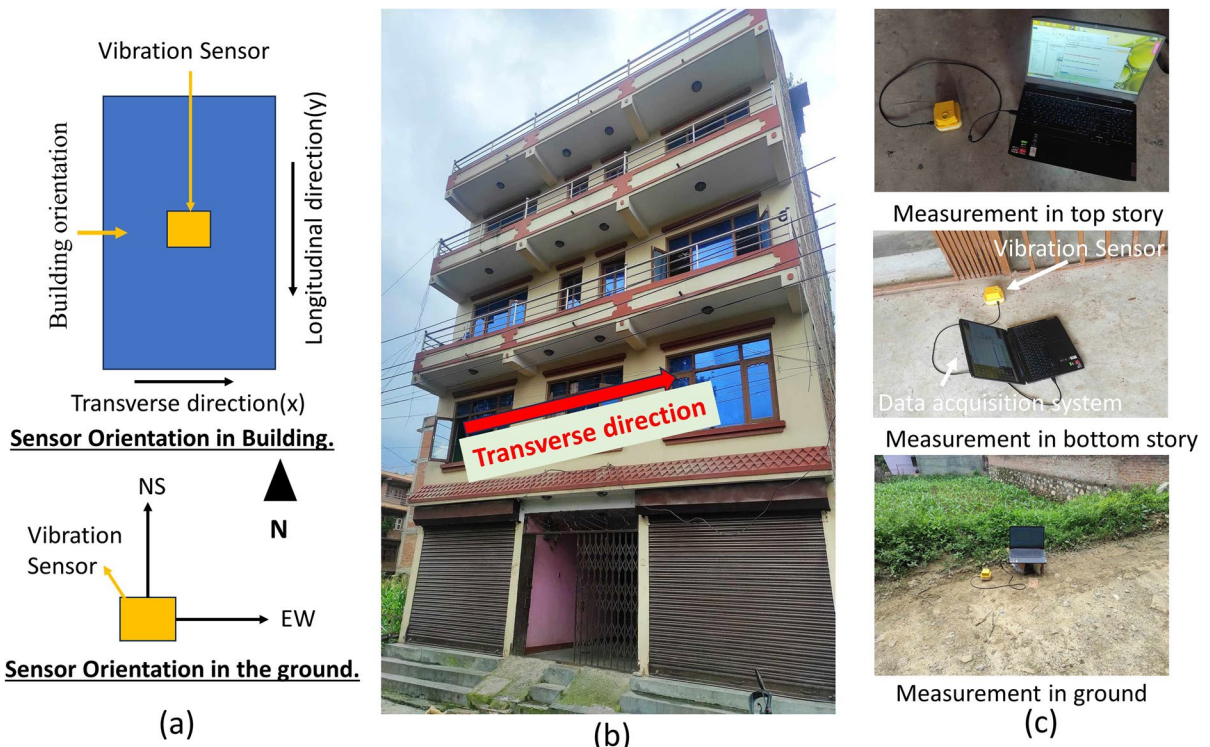


Fig. 5 Typical microtremor measurement: **a** orientation of microtremor measurement in plan view of the building and ground, **b** typical isolated RCC building (BU3), and **c** microtremor recording on the top floor, bottom floor, and ground point

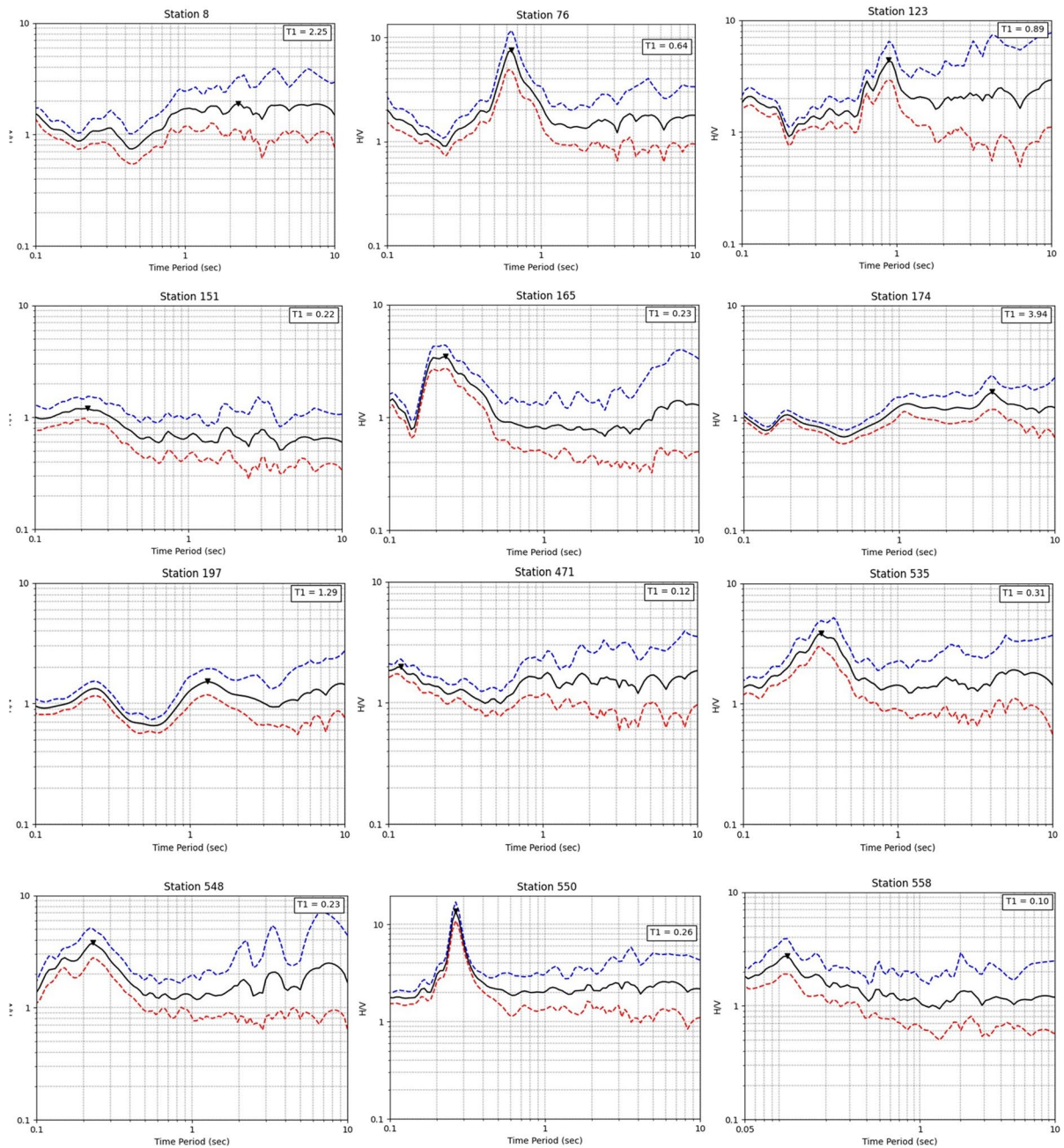


Fig. 6 Some representative HVSr graphs of measurement stations of the study area. Solid lines represent the average HVSr curve. The dotted lines represent a 95% confidence interval of the average HVSr curve

the aforementioned criteria. About 14% of the stations that did not meet the criteria were omitted and were not taken into account in the micro-zonation mapping. Different types of HVSr frequency peaks, as shown in Fig. 6, were obtained from the analysis

of microtremor data—clear low- and high-frequency peaks, multiple frequency peaks, broad peaks, and flat H/V curves. The previous investigation (Gallipoli et al. 2004b; Mukhopadhyay and Bormann 2004; Gosar 2010; Herak 2011; Paudyal et al. 2012b, a)

also demonstrates similar findings to the frequency peaks and HVSR amplitude. These HVSR curves indicate that the study area has heterogeneous sub-surface soil. The southernmost region of the study area mostly exhibits a clear low period and distinct HVSR peaks—typical examples of this type of HVSR observed in station 76, station 123, station 165, and station 550 are shown in Fig. 6. The low period of the site is caused by shallow sediments layer over the bedrock, whereas clear HVSR peaks are due to significant impedance contrast between sediment and bedrock beneath. Some flat HVSR curves were also observed in the southern parts, possibly due to stiff sediment deposits over bedrock or the rocky area. A few flat HVSR curves obtained at stations 151, 471, and 558 are depicted in Fig. 6. The western and central regions of the research area primarily experienced high periods with flat HVSR curves and a few multiple peaks. The HVSR curves of station 8, station 174, station 197, and station 265 are some illustrative examples of this kind, as shown in Fig. 6. The flat HVSR curve and low amplitude are observed due to the low impedance contrast between sediments deposits (stiff) and underlying bedrock, whereas the multiple peaks in HVSR graph indicate multiple soil layers with significant variations in the density and shear wave velocity between the layers. Similar to the southern part, in the northern part of the study area, clear low period and flat HVSR curves

were observed. This result indicates that the clear low period and flat HVSR curves were prominent near the edges of the study area (stations 550, 558, and 537 in Fig. 6), except in the western part of the study area. These observed HVSR curve results strongly correlate with the stratigraphic fencing diagram provided by Kawan et al. (2019), which is shown in Fig. 7. From Fig. 7, it can be observed that in the central part of the study area, the soft sediment deposit over rock strata is thick, whereas in the surrounding part of the study area, the soft sediment deposit is of shallow depth over rock strata.

Figure 8 illustrates the period-based microzonation map of the Bhaktapur district prepared in the GIS environment using 609 measured points. The study area is categorized into four different ranges: A (0.10–0.6 s), B (0.6–1.0 s), C (1.0–1.7 s), and D (1.7–4.0 s). Moving from the Western to the Eastern edge, the dominant period declines towards the eastern side until it reaches the boundary between Bhaktapur and Madhyapur Thimi municipality. As it shifts towards the eastern side, the period rises yet again, eventually ending with a low period at the eastern margins. On the other hand, moving from the northeast (NE) to southeast (SE), it can be observed that the period value increases in the middle portion of the study area and decreases in the edges of the study areas. This indicates that the central and the western portions of the study area have a

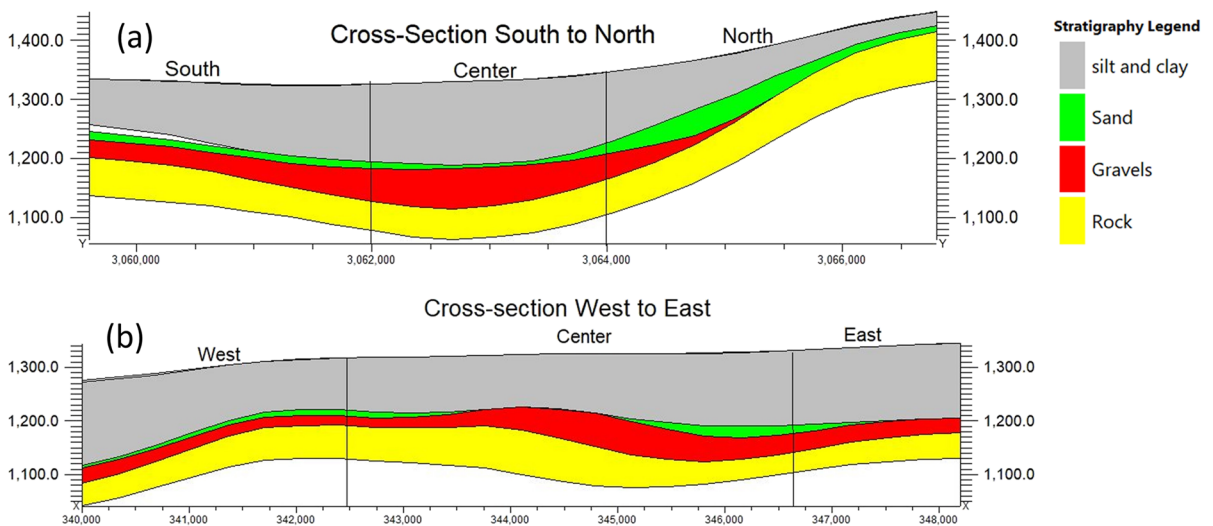


Fig. 7 2-D stratigraphic fencing diagram of Bhaktapur: **a** stratigraphic soil profile mid-way from south to north; **b** stratigraphic soil profile mid-way from west to east (Kawan et al. 2019)

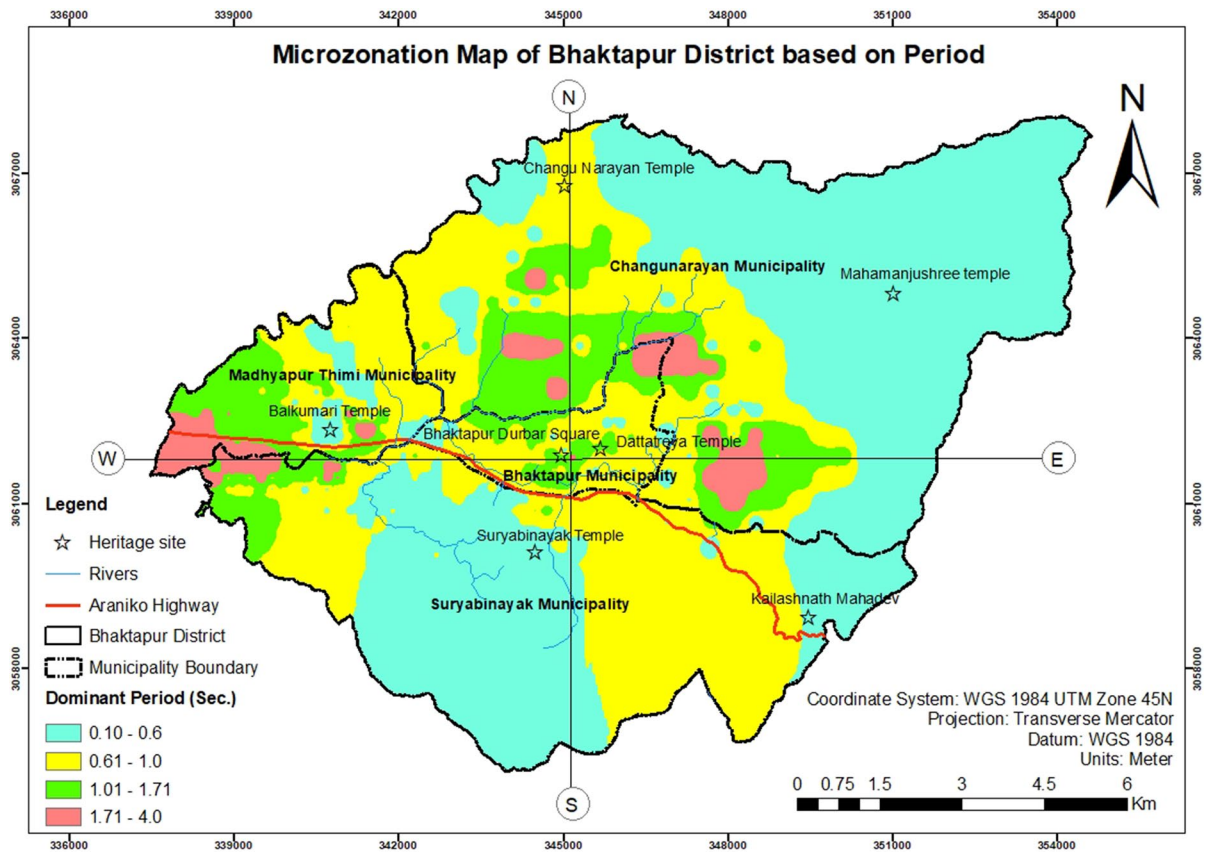


Fig. 8 Period-based microzonation of Bhaktapur district (scale 1:75,000)

high ground period compared to the surrounding other parts of the study areas. The result shows the highland topography (eastern, northern, and southern part of the study areas) has the lowest period range A. This result was reasonably anticipated as the sediment deposited, Pilo-Pleistocene and recent quaternary, in the central portion of the study area is higher compared to the surrounding parts as shown in Fig. 7. Kawan et al. (2019, 2022a) had shown that soil sediment in the central area of the study area goes up to 350 m, which is limited to the 15 m near the southern and northern boundary areas of the study area (Fig. 7).

The map also depicts the UNESCO World Heritage sites and some of the historically important temples of the Bhaktapur district. The Bhaktapur Durbar Square and Changuarayan are enlisted as world heritage sites of the Bhaktapur district. The Bhaktapur Durbar square and some well-known temples like Nyatapola Temple and Dattatraya Temple

of Bhaktapur municipality fall within category C (1.01–1.7 s). These sites were expected to have a comparatively higher period due to the considerable depth of the soft sediment layers (Kalimati) over the bedrock. Similarly, the Changuarayan Temple, one of the oldest temples in Nepal erected in the fourth century and recognized as a UNESCO World Heritage site in 1979 A.D., is located in the northern portion of the study area (Changuarayan municipality). These sites fall within the B (0.6–1.0) range due to the shallow depth of the silt layer over the bedrock. The Balkumari Temple, built in the seventeenth century in the oldest settlement of Madhyapur Thimi municipality, lies in range A (0.10–0.6 s). The Suryabinayak Temple was also built in the seventeenth century and lies in the Suryabinayak municipality, falling in range A (0.10–0.6 s). This temple is located in the southernmost part of the study area, where the depth of the soil over the rock strata is thin.

4.2 Soil-structure resonance

From the microtremor measurement done in the buildings, floor spectral ratio (FSR) plots were obtained, and the representative FSR plots for four different locations are shown in Fig. 9. The building’s fundamental period corresponds to the clear isolated peaks in FSR for both directions. Table 1 summarizes the fundamental period of the measured buildings. From Table 1, it can be observed that the transverse period is generally longer than the longitudinal period, possibly due to the higher stiffness in the longitudinal direction. In most of square configuration buildings, the fundamental periods obtained from longitudinal and transverse FSR show no significant difference. This result was anticipated as the distribution of columns in both directions is the same. With an increment in the building height or number of stories, the predominant periods of the buildings also increased. The fundamental period of

the measured buildings in the study area ranges from 0.12 to 0.42 s.

These obtained predominant periods were also compared with the empirical relation given by Kramer (1996). Kramer (1996) suggests that the natural period (T) of an N -story reinforced concrete structure can be obtained using the empirical relation: $T=0.1 N$. The surveyed building’ stories vary from 2 to 5, and using the empirical equation, the calculated fundamental periods vary from 0.2 to 0.5 s, which is higher than the measured periods as shown in Fig. 10. This comparison indicates that except for a few buildings, the predominant periods obtained from the microtremor measurement are lower than those obtained from the empirical equation. Similar results were also found by Al-Nimry et al. (2014) and Bhandary et al. (2021) in their studies. The time period obtained from the experiment was further compared with the Nepal Building Code (NBC)105:2020. Figure 10b illustrates the linear

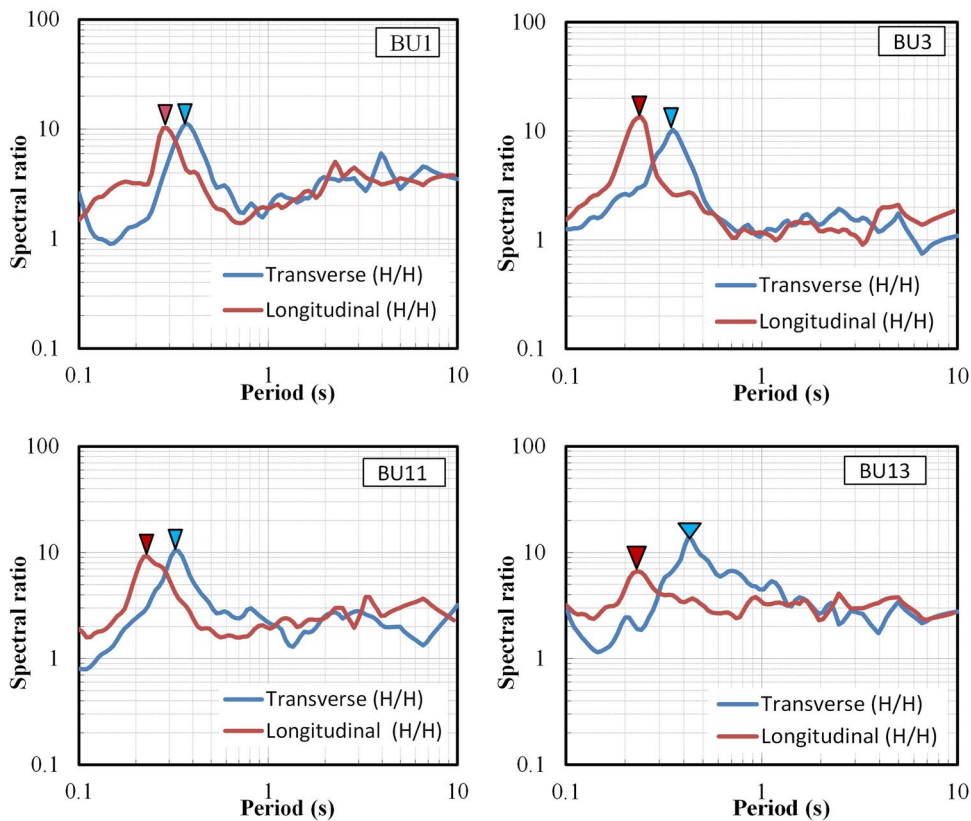


Fig. 9 Floor spectral ratio of the buildings located at four different places of the municipalities (buildings’ locations are indicated in Fig. 12)

Table 1 Features of surveyed buildings with soil-structure resonance possibility

New building ID	No. of story	Number of bays	Buildings period (sec)		Free-field period	Percentage difference (%)	Level of danger
			Longitudinal period	Transverse period			
BU1	4	2×4	0.27	0.36	0.24	52.07	High
BU2	2	2×2	0.12	0.13	1.30	89.78	Low
BU3	5	2×3	0.24	0.35	0.35	0.00	High
BU4	5	3×3	0.27	0.30	0.85	64.78	Low
BU5	4	2×3	0.27	0.27	0.57	52.63	Low
BU6	2	2×3	0.13	0.13	0.17	25.54	Medium
BU7	3	2×2	0.21	0.26	0.53	50.86	Low
BU8	3	2×3	0.15	0.17	0.70	75.07	Low
BU9	2	2×2	0.15	0.12	0.93	87.10	Low
BU10	5	2×4	0.19	0.35	0.40	11.97	High
BU11	4	3×3	0.22	0.31	1.30	75.81	Low
BU12	5	2×3	0.18	0.14	0.59	76.27	Low
BU13	5	2×3	0.23	0.42	0.89	52.81	low
BU14	3	2×3	0.15	0.15	1.54	90.25	Low
BU15	4	2×3	0.22	0.38	0.35	9.34	High
BU16	5	3×3	0.25	0.26	0.93	72.14	Low
BU17	3	3×3	0.19	0.18	0.89	79.42	Low
BU18	2	2×2	0.14	0.15	0.20	23.90	Medium
BU19	2	2×4	0.14	0.15	0.15	3.24	High
BU20	3	2×3	0.22	0.26	1.30	80.00	Low
BU21	4	2×3	0.28	0.31	0.35	12.63	High
BU22	3	2×3	0.23	0.20	0.74	72.97	Low
BU23	4	3×3	0.22	0.23	0.62	63.26	low
BU24	2	2×3	0.13	0.15	0.85	81.84	Low
BU25	5	2×2	0.24	0.34	1.85	81.62	Low
BU26	4	2×3	0.18	0.16	0.53	69.81	Low
BU27	3	1×3	0.17	0.19	1.00	81.00	Low
BU28	3	2×2	0.22	0.21	1.47	85.71	Low

regression line between the predominant period (longitudinal and transverse period) and the height of the buildings. It can be observed from Fig. 10b that the period acquired from the ambient vibration test is lower than that from the codal provisions, consistent with research undertaken by several researchers, including Chiauzzi et al. (2012), Hong and Hwang (2000), Shrestha and Karanjit (2017), Gallipoli et al. (2020), and Gangone et al. (2023). The lower value of time from experimental provisions compared to codal provisions may be attributed to the stiffness of the infill wall and non-structural elements of the building. These studies justify the results of the predominant periods of the buildings obtained in the study area. In

Fig. 10, it can also be observed that the predominant periods for the same story number are also different. This is also obvious because the predominant period of a building is affected by the source of incoming waves in the building, the structural plan of the building, structural components, construction material, building orientation, the center of mass, floor height, and year of construction (Naito and Ishibashi 1996; Bhandary et al. 2021).

To understand the possibility of soil-structure resonance conditions of the surveyed buildings, the floor spectral ratios obtained for all the buildings were compared with the H/V spectral ratios obtained from free-field measurements at nearby locations. If the

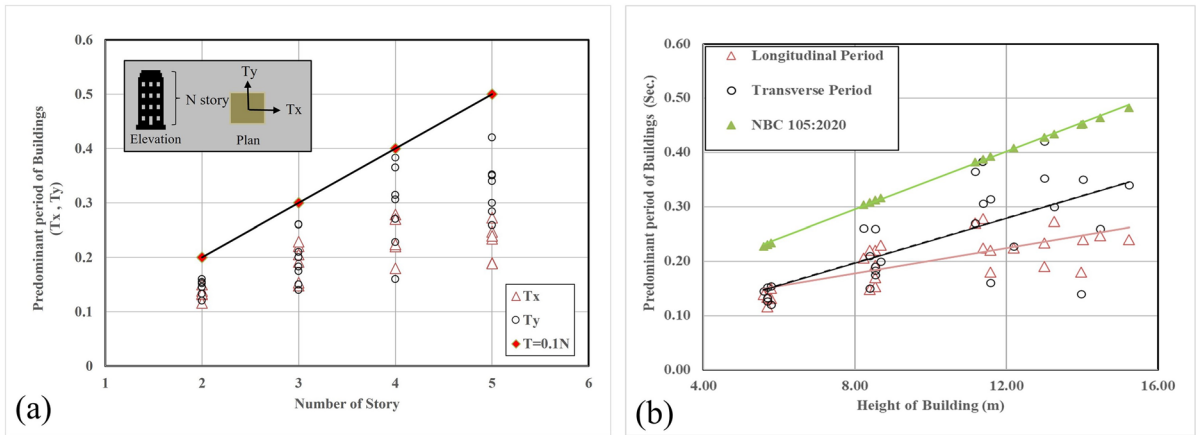


Fig. 10 Comparison of predominant periods of the buildings obtained from microtremor measurements with **a** the natural periods obtained from Kramer (1996) (Kramer 1996) and **b** the natural periods obtained from NBC105:2020

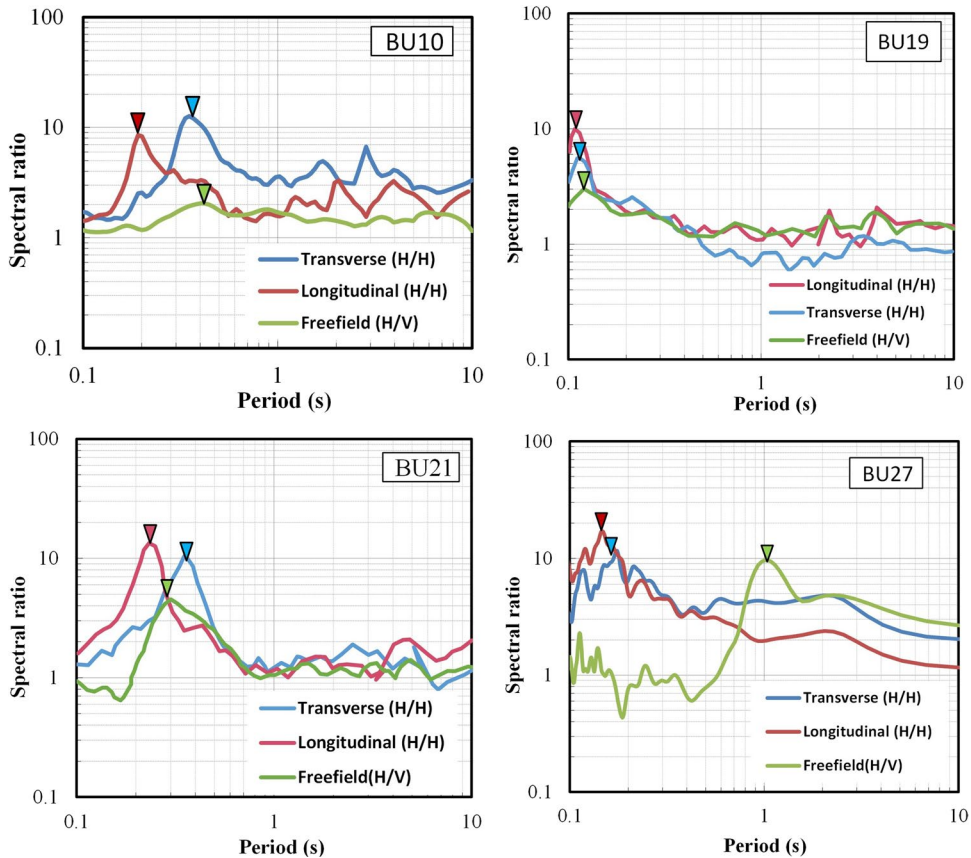


Fig. 11 Comparison of spectral ratios obtained for buildings (FSR) and free-field (HVSr), the location of the building is shown in Fig. 12

time period of the building is close to the time period of the free-field, a potential resonance between the soil and structure is considered, which may result in significant damage to structures (Gosar et al. 2010). From Fig. 11, it can be noticed that buildings 10, 19, and 21 are in resonance conditions with free-field, whereas building 27 is safe from resonance conditions. The severity of soil-structure resonance was computed using the relationship given by Gosar (2010) and Stanko et al. (2017):

$$\text{FSR (\%)} = \frac{|T_{\text{building}} - T_{\text{freefield}}|}{T_{\text{freefield}}} \dots \quad (1)$$

Stanko et al. (2017) and Gosar (2010) suggest that the severity of soil structure is high if the FSR (%) is within $\pm 15\%$, medium if it is between $\pm 15\%$ and $\pm 25\%$, and low if it is greater than $\pm 25\%$. In Eq. (1), T_{building} and $T_{\text{freefield}}$ denote the fundamental period of the building and free-field, respectively. In Eq. (1), out of two directional periods of the building

(longitudinal and transverse), the period with higher susceptibility to soil-structure is used for the calculation of FSR (%). From Table 1, it can be observed that the difference between the period of the free-fields and buildings for BU1, BU3, BU10, BU15, BU19, and BU21 lies within $\pm 15\%$. This indicates that these buildings are at high risk of soil-structure resonance conditions. A building's high susceptibility to soil-structure resonance may cause damage during seismic events, alongside numerous other factors such as construction methods, quality of material, and workmanship. The isolated reinforced concrete (RC) buildings BU15 and BU19 in the Suryabinayak Municipality, BU10 in the Madhyapur Municipality, BU1 in the Changunaryan, and BU3 in the Bhaktapur Municipality were built in compliance with building codes and bye-laws. So, despite a high likelihood of soil-structure resonance, these buildings are expected to suffer little damage during seismic events. BU1 and BU21 are somewhat older buildings. Therefore, these buildings could sustain

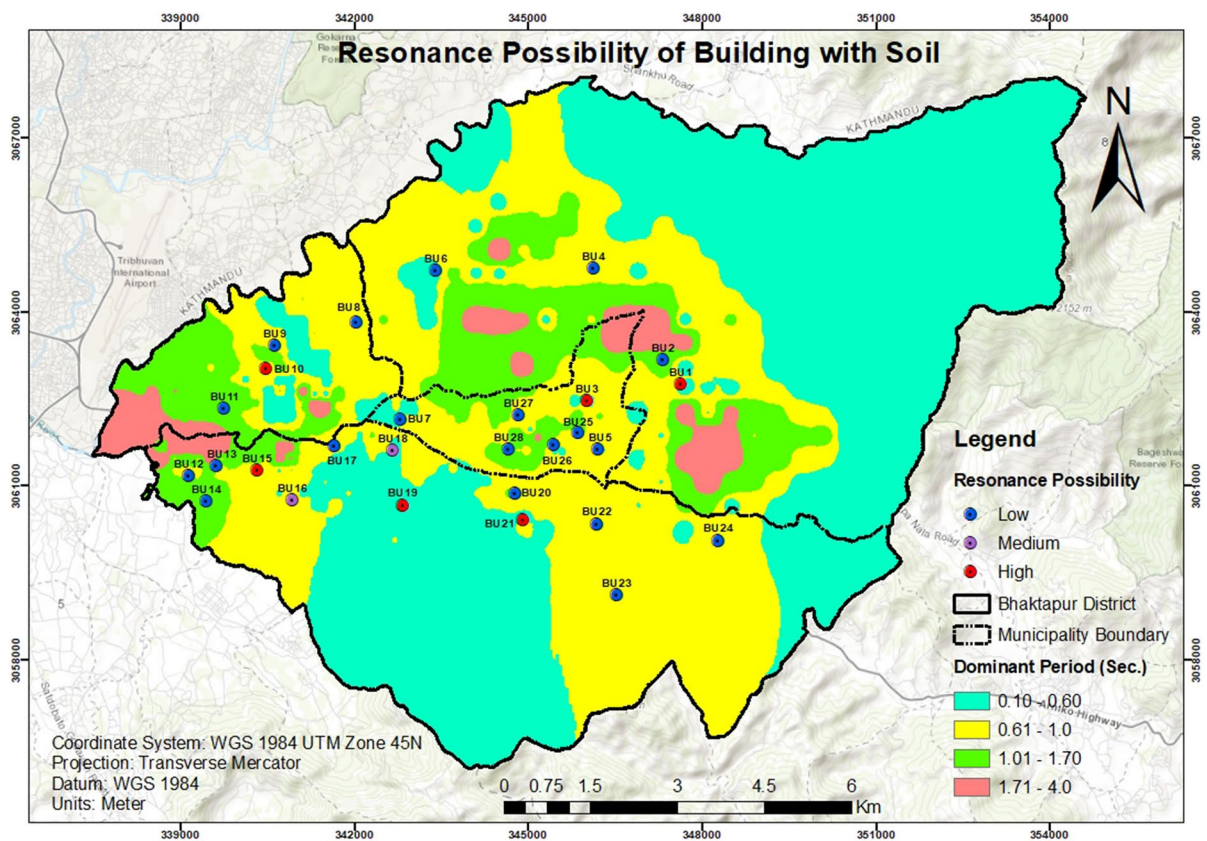


Fig. 12 Showing the level of danger of surveyed buildings with relation to soil-structure resonance

significant damage during earthquakes. These buildings survived the 2015 Gorkha earthquake with minor non-structure damages. Moreover, BU6 and BU18 have an FSR (%) value of 25.54% and 23.90%, lying between $\pm 15\%$ and 25% , indicating the medium severity of the building due to soil-structure resonance conditions. The remaining buildings are characterized by a low level of soil-structure resonance, as the percentage difference between structure and free-field period is greater than $\pm 25\%$. The degree of risk resulting from the resonance condition of soil and structure is depicted in the spatial predominant period map using different color codes as given in Fig. 12.

5 Conclusion

Seismic hazard mitigation is a major concern in the seismic zones for the protection of the livelihoods and properties of the people. In this study, the microtremor HVSR method was used to determine the predominant period of the ground and prepare a seismic hazard map, which can be utilized for seismic hazard mitigation measures. The study also aimed to understand the possibility of soil-structure resonance. The microtremor measurements were conducted with a grid spacing of $200\text{ m} \times 200\text{ m}$ in the core city areas and $400\text{ m} \times 400\text{ m}$ on the outskirts, totaling 609 measurement points. The spatial distribution map of the predominant period reveals a range from 0.1 to 4 s in the study area, with longer periods in the central and eastern parts compared to the surrounding areas. Periods in the central portion range from 0.6 to 0.4 s, with a few areas ranging from 1.7 to 4.0 s. As the central parts are densely populated, precautions need to be taken during construction to avoid the resonance between structures and the ground. The microtremor measurements were also conducted in 28 isolated reinforced buildings to assess the danger level of soil-structure resonance. The predominant period of these buildings ranges from 0.12 to 0.42 s. The assessment reveals that out of 28 surveyed buildings, six have a high possibility, two buildings have medium possibility, and 20 have a low possibility of soil-structure resonance. This result highlights the potential structural damage due to soil-structure resonance in the study area, emphasizing the importance of seismic hazard

mitigation measures, earthquake-resilient construction practices, and the preservation of heritage sites.

It should be noted that the soil-structure resonance map presented in this study is limited to the interaction effect in the linear-elastic domain, and the offered resonance map could be altered when considering strong ground motion. This is because the proposed microtremor method only works under weak motions. Strong ground shaking can shift the fundamental frequency of the soil sediment and the building due to the consequences of damage. Therefore, this study can be extended by creating a soil-structure resonance map and seismic risk map considering strong ground motions. The microzonation map based on soil-structure resonance frequency is also essential for urban areas because such a map will aid in seismic mitigation, urban planning, and retrofitting and restrengthening of existing important structures. In this study, the ground response analysis is conducted using ambient vibration tests, with certain limitations. For a better evaluation of the response of soil sediment, analytical methods, such as one-dimensional site response or even two- or three-dimensional site response analysis, can be conducted, which can also serve to validate the results obtained from the experimental method. To assess the seismic risk in urban areas, the characterizing buildings in terms of fundamental periods, built configuration, structural characteristics, and foundation soil types is essential. These parameters of the built environment need to be acquired in future works for seismic risk assessment. Additionally, in this study, fundamental frequencies of the building were obtained using microtremor measurements. These obtained fundamental frequencies can be used to generate empirical relations, such as time (T) versus height (H). The developed relation can then be used to obtain the fundamental frequencies of other buildings, which will further aid in developing a comprehensive and more precise soil-structure resonance hazard map.

Acknowledgements We are grateful to Dr. Manjip Shakya, Dr. Subeg Man Bijukchhen, and Sudip Karanjit of the post-graduate earthquake department at Khwopa Engineering College for their guidance and technical support in the microtremor survey. We would also like to express our gratitude to Principal Sunil Duwal of Khwopa College of Engineering for his administrative support. Lastly, sincere acknowledgment to the University Grant Commission (UGC), Bhaktapur, Nepal for their financial aid.

Author contributions The field instrumental measurements were carried out under the lead of Dinesh Sakhakarmi and Amit Prajapati. The acquired data were processed by Chandra Kiran Kawan and Dinesh Sakharami. Most of the figures were prepared by Dinesh Sakhakarmi and Amit Prajapati. The manuscript was written by Chandra Kiran kawan.

Funding This work was supported by the University Grant Commission (UGC), Bhaktapur, Nepal (FRG-77/78-Engg-3).

Data availability All the data and materials used are mentioned in the manuscript.

Declarations

Competing interests The authors declare no competing interests.

References

- Al-Nimry H, Resheidat M, Al-Jamal M (2014) Ambient vibration testing of low and medium rise infilled RC frame buildings in Jordan. *Soil Dynamics Earthquake Eng* 59. <https://doi.org/10.1016/j.soildyn.2014.01.002>
- Bhandary NP, Paudyal YR, Okamura M (2021) Resonance effect on shaking of tall buildings in Kathmandu Valley during the 2015 Gorkha earthquake in Nepal. *Environ Earth Sci* 80. <https://doi.org/10.1007/s12665-021-09754-9>
- Bijukchhen SM (2018) Construction of 3-D velocity structure model of the Kathmandu Basin, Nepal, based on geological information and earthquake ground motion records. PhD dissertation, Hokkaido University
- Bindi D, Petrovic B, Karapetrou S, Manakou M, Boxberger T et al (2015) Seismic response of an 8-story RC-building from ambient vibration analysis. *Bull Earthq Eng* 13:2095–2120
- Bonnefoy-Claudet S, Baize S, Bonilla LF et al (2009) Site effect evaluation in the basin of Santiago de Chile using ambient noise measurements. *Geophys J Int* 176:925–937. <https://doi.org/10.1111/j.1365-246X.2008.04020.x>
- Castro RR, Ruiz E, Uribe A, Rebolgar CJ (2000) Site response of the Dam El Infiernillo. Guerrero-Michoacan, Mexico
- Chiauzzi L, Masi A, Mucciarelli M, Cassidy JF, Kutyn K, Traber J, Ventura C, Yao F (2012) Estimate of fundamental period of reinforced concrete buildings: code provisions vs. experimental measures in Victoria and Vancouver (BC, Canada). In the Proceeding of 15th World Conference on Earthquake Engineering vol 3033
- D'Alessandro A, Luzio D, Martorana R, P. Capizzi P, (2016) Selection of time windows in the horizontal-to-vertical noise spectral ratio by means of cluster analysis. *Bull Seismol Soc Am* 106(2):560–574. <https://doi.org/10.1785/0120150017>
- Department of Mines and Geology (DMG) (1998) Engineering and environmental geology map of Kathmandu Valley. Department of Mines and Geology, Kathmandu, Nepal
- Field E, Jacob K (1993) The theoretical response of sedimentary layers to ambient seismic noise. *Geophys Res Lett* 20. <https://doi.org/10.1029/93GL03054>
- Gallipoli MR, Mucciarelli M, Ponzio F, Dolce M, D'Alema E, Maistrello M (2006) Buildings as a seismic source: analysis of a release test at Bagnoli, Italy. *Bull Seismol Soc Am* 96(6):2457–2464
- Gallipoli MR, Calamita G, Tragni N, Pisapia D, Lupo M et al (2020) Evaluation of soil-building resonance effect in the urban area of the city of Matera (Italy). *Eng Geol* 272:105645
- Gallipoli MR, Mucciarelli M, Castro RR et al (2004a) Structure, soil-structure response and effects of damage based on observations of horizontal-to-vertical spectral ratios of microtremors. *Soil Dynamics Earthquake Eng* 24. <https://doi.org/10.1016/j.soildyn.2003.11.009>
- Gallipoli MR, Mucciarelli M, Gallicchio S et al (2004b) Horizontal to vertical spectral ratio (HVSr) measurements in the area damaged by the 2002 Molise, Italy, earthquake. *Earthquake Spectra* 20. <https://doi.org/10.1193/1.1766306>
- Gangone G, Gallipoli MR, Tragni N, Vignola L (2023) Caputo R (2023) Soil-building resonance effect in the urban area of Villa d'Agri (Southern Italy). *Bull Earthq Eng* 21:3273–3296. <https://doi.org/10.1007/s10518-023-01644-8>
- García-Fernández M, Jiménez MJ (2012) Site characterization in the Vega Baja, SE Spain, using ambient-noise HV analysis. *Bull Earthq Eng* 10:1163–1191. <https://doi.org/10.1007/s10518-012-9351-1>
- Gilder CEL, Pokhrel RM, Vardanega PJ et al (2020) The SAFER geodatabase for the Kathmandu Valley: geotechnical and geological variability. *Earthquake Spectra* 36. <https://doi.org/10.1177/8755293019899952>
- Giocoli A, Hailemichael S, Bellanova J, Calamita G, Perrone A, Piscitelli S (2019) Site and building characterization of the Orvieto Cathedral (Umbria, Central Italy) by electrical resistivity tomography and single-station ambient vibration measurements. *Eng Geol* 260:105195
- Gosar A, Martinec M (2008) Microtremor HVSr study of site effects in the Ilirska Bistrica Town Area (S. Slovenia). *J Earthquake Eng* 13:50–67. <https://doi.org/10.1080/13632460802212956>
- Gosar A, Rošar J, Motnikar BŠ, Zupančič P (2010) Microtremor study of site effects and soil-structure resonance in the city of Ljubljana (central Slovenia). *Bull Earthq Eng* 8:571–592. <https://doi.org/10.1007/s10518-009-9113-x>
- Gosar A (2010) Site effects and soil-structure resonance study in the Kobarid basin (NW Slovenia) using microtremors. *Nat Hazards Earth Syst Sci* 10(4):761–772. <https://doi.org/10.5194/nhess-10-761-2010>
- Gosar A (2012) Determination of masonry building fundamental frequencies in five Slovenian towns by microtremor excitation and implications for seismic risk assessment. *Nat Hazards* 62. <https://doi.org/10.1007/s11069-012-0138-0>
- Gueguen P, Bard PY, Oliveira CS (2000) Experimental and numerical analysis of soil motions caused by free vibrations of a building model. *Bull Seismol Soc Am* 90(6):1464–1479
- Herak M (2011) Overview of recent ambient noise measurements in Croatia in free-field and in buildings. *Geofizika* 28:21–40

- Hong L, Hwang W (2000) Empirical formula for fundamental vibration periods of reinforced concrete buildings in Taiwan. *Earthquake Eng Struct Dynam* 29:327–337
- Horike M, Zhao B, Kawase H (2001) Comparison of site response characteristics inferred from microtremors and earthquake shear waves. *Bull Seismol Soc Am* 81:1526–1536
- Irie Y, Nakamura K (2000) Dynamic characteristics of ar/c building of five stories based on microtremor measurements and earthquake observations. In 12th World Conference on Earthquake Engineering, Auckland Australia
- Kanamori H, Mori J, Anderson DL, Heaton TH (1991) Seismic excitation by the space shuttle Columbia. *Nature* 349(6312):781–782
- Kawan CK, Maskey PN, Motra GB (2022a) A study of local soil effect on the earthquake ground motion in Bhaktapur City, Nepal using equivalent linear and non-linear analysis. *Iran J Sci Technol - Trans Civil Eng* 46:4481–4498. <https://doi.org/10.1007/s40996-022-00858-1>
- Kawan CK, Maskey PN, Motra GB (2022b) Dynamic characterization of high plinths of temples in the Kathmandu valley using microtremors. *Int J Archit Herit* 16:645–666. <https://doi.org/10.1080/15583058.2020.1833107>
- Kawan CK, Maskey PN, Motra G (2019) Spatial variation of silt and clay sediment deposit in Bhaktapur city. *Journal of Science and Engineering* 7
- Koller MG, Chatelain J, Gullier B, Duval A, Atakan K, Lacave C, Bard P, and Sesame Participants (2004) Practical user guidelines and software for the implementation of the H/V ratio technique: measuring conditions, processing method, and results interpretation. In proceeding of the 13th World Conference in Earthquake Engineering, Vancouver
- Konno K, Ohmachi T (1998) Ground-motion characteristics estimated from spectral ratio between horizontal and vertical components of microtremor. *Bull Seismol Soc Am* 88(1):228–241
- Kramer SL (1996) Geotechnical earthquake engineering. In: Hall WJ (eds) Upper Saddle River, NJ: Prentice-Hall International Series in Civil Engineering and Engineering Mechanics
- Laurenzano G, Priolo E, Gallipoli MR, Mucciarelli M, Ponzio FC (2010) Effect of vibrating buildings on free-field motion and on adjacent structures: the Bonefiro (Italy) case history. *Bull Seismol Soc Am* 100(2):802–818
- Lermo J, Chávez-García FJ (1993) Site effect evaluation using spectral ratios with only one station. *Bull Seismol Soc Am* 83:1574–1594
- Lermo J, Chávez-García FJ (1994) Are microtremors useful in site response evaluation? *Bull Seismol Soc Am* 84:1350–1364
- McGowan SM, Jaiswal KS, Wald DJ (2017) Using structural damage statistics to derive macroseismic intensity within the Kathmandu valley for the 2015 M7.8 Gorkha, Nepal earthquake. *Tectonophysics* 714–715. <https://doi.org/10.1016/j.tecto.2016.08.002>
- Ministry of Home Affairs (MoHA) (2015) Nepal earthquake 2015: Situation updates as of 11st May. <http://drrpo.rta.gov.np/uploads/document/14.pdf>
- Moisidi M, Vallianatos F, Kershaw S, Collins P (2015) Seismic site characterization of the Kastelli (Kissamos) Basin in northwest Crete (Greece): assessments using ambient noise recordings. *Bull Earthq Eng* 13:725–753. <https://doi.org/10.1007/s10518-014-9647-4>
- Moisidi M, Vallianatos F, Makris J et al (2004) Estimation of seismic response of historical and monumental sites using microtremors: a case study in the ancient Aptera, Chania, (Greece). *Bull Geol Soc Greece* 36
- Moribayashi S, Maruo Y (1980) Basement topography of the Kathmandu Valley, Nepal - an application of gravitational method to the survey of a tectonic basin in the Himalayas. *J Jpn Soc Eng Geol* 21. <https://doi.org/10.5110/jjseg.21.80>
- Mucciarelli M, Gallipoli MR (2001) A critical review of 10 years of microtremor HVSR technique. *Boll Geof Teor Appl* 42:255–266
- Mucciarelli M, Contri P, Monachesi G et al (2001) An empirical method to assess the seismic vulnerability of existing buildings using the HVSR technique. *Pure Appl Geophys* 158:2635–2647. <https://doi.org/10.1007/PL00001189>
- Mucciarelli M, Gallipoli MR (2004) The HVSR technique from microtremor to strong motion: empirical and statistical considerations. In: Proc. of 13th World Conference of Earthquake Engineering, vol 45. Vancouver, Canada, Paper
- Mucciarelli M, Monachesi G (1998) A quick survey of local amplifications and their correlation with damage observed during the Umbro-marchesano (Italy) earthquake of September 26, 1997. *J Earthquake Eng* 2. <https://doi.org/10.1080/13632469809350325>
- Mucciarelli M, Bettinali F, Zaninetti M, Vanini M, Mendez A et al (1996) Refining Nakamura's technique: processing techniques and innovative instrumentation. In Proceedings of ESC Assembly, Reykjavik, pp. 411–416
- Mukhopadhyay S, Bormann P (2004) Low cost seismic microzonation using microtremor data: an example from Delhi, India. *J Asian Earth Sci* 24:271–280. <https://doi.org/10.1016/j.jseae.2003.11.005>
- Naito Y, Ishibashi T (1996) Identification of structural systems from microtremors and accuracy factors. In: Eleventh World Conference on Earthquake Engineering, Paper, pp 770
- Nakamura Y (1989) A method for dynamic characteristics estimation of subsurface using microtremor on the ground surface. *Q Rep Railw Tech Res Inst (RTRI)* 30:25–33
- Nakamura Y, Gurler ED, Saita J (1999) Dynamic characteristics of leaning tower of Pisa using microtremor. In Proceedings of the JSCE earthquake engineering symposium, vol 25. Japan Society of Civil Engineers, pp 921–924
- Nakamura Y, Gurler ED, Saita J, Rovelli A, Donati S (2000) Vulnerability investigation of Roman Colosseum using microtremor. Proceeding, 12th WCEE, pp 1–8
- Natale M, Nunziata C (2004) Spectral amplification effects at Sellano, Central Italy, for the 1997–98 Umbria seismic sequence. *Nat Hazards* 33. <https://doi.org/10.1023/B:NHAZ.0000048463.15620.86>
- Nogoshi M, Igarashi T (1970) On the propagation characteristics of microtremors. *J Seismol Soc Jpn* 23:264–80
- Nogoshi M, Igarashi T (1971) On the amplitude characteristics of microtremors. *J Seismol Soc Jpn* 24:26–40
- Ohmachi T, Konno K, Endoh T, Toshinawa T (1994) Refinement and application of an estimation procedure for site natural periods using microtremor. *J Jsee* 489:251–261
- Pandey MR, Molnar P (1988) The Distribution of Intensity of the Bihar_Nepal earthquake of 15 January 1934 and bounds of the extent of the rupture zone. *J Nepal Geol Soc* 5:22–44

- Pandey MR (2000) Ground response of Kathmandu Valley on the basis of microtremors. In: Proceedings of the 12th world conference on earthquake engineering, Auckland, New Zealand vol 30
- Panou A, Theodulidis N, Hatzidimitriou P et al (2005) Ambient noise horizontal-to-vertical spectral ratio in site effects estimation and correlation with seismic damage distribution in urban environment: the case of the city of Thessaloniki (Northern Greece). *Soil Dyn Earthq Eng* 25:261–274
- Parajuli HR, Bhusal B, Paudel S (2021) Seismic zonation of Nepal using probabilistic seismic hazard analysis. *Arab J Geosci* 14. <https://doi.org/10.1007/s12517-021-08475-4>
- Parolai S, Fäcke A, Richwalski SM, Stempniwski L (2005) Assessing the vibrates of the Holweide Hospital in the City of Cologne (Germany) by means of ambient seismic noise analysis and FE modelling. *Nat Hazards* 34. <https://doi.org/10.1007/s11069-004-0686-z>
- Parolai S, Picozzi M, Strollo A, Pilz M, Di Giacomo D, Liss B, Bindi D (2009) Are transients carrying useful information for estimating H/V spectral ratios? In: Increasing Seismic Safety by Combining Engineering Technologies and Seismological Data, Mucciarelli M (Editor) Proc. of the NATO Advanced Research Workshop, NATO Science for Peace and Security Series: C: Environmental Security, Springer, 17–31
- Parolai S, Galiana-Merino JJ (2006) Effects of transient seismic noise on estimates of H/V spectral ratios. *Bull Seismol Soc Am* 96(1):228–236
- Paudyal KN (2015) New discovery of late pleistocene vertebrate fossils from the Thimi Formation, Bhaktapur, Nepal. *J Instr Sci Technol* 20(2):73–75
- Paudel MR, Sakai H (2008) Stratigraphy and depositional environments of basin-fill sediments in southern Kathmandu Valley, Central Nepal. *Bull Dep Geol* 11:61–70
- Paudyal YR, Bhandary NP, Yatabe R (2012a) Seismic microzonation of densely populated area of Kathmandu Valley of Nepal using microtremor observations. *J Earthquake Eng* 16:1208–1229
- Paudyal YR, Yatabe R, Bhandary NP, Dahal RK (2012b) A study of local amplification effect of soil layers on ground motion in the Kathmandu Valley using microtremor analysis. *Earthquake Eng Eng Dynamics* 11:257–268. <https://doi.org/10.1007/s11803-012-0115-3>
- Petrovic B, Parolai S (2016) Joint deconvolution of building and downhole strong-motion recordings: evidence for the seismic wavefield being radiated back into the shallow geological layers. *Bull Seismol Soc Am* 106(4):1720–1732
- Piya BK (2004) Generation of a geological database for the liquefaction hazard assessment in Kathmandu Valley. Master thesis, ITC
- Bhandary NP, Yatabe R, Yamamoto K, Paudyal YR (2014) Use of a Sparse Geo-Info Database and ambient ground vibration survey in earthquake disaster risk study- A case of Kathmandu Valley. *J Civ Eng Res* 4(3A):20–30
- Rajaure S (2021) Seismic hazard assessment of the Kathmandu Valley and its adjoining region using a segment of the main Himalayan Thrust as a source. *Prog Disaster Sci* 10. <https://doi.org/10.1016/j.pdisas.2021.100168>
- Sakai H (2001) Stratigraphic division and sedimentary facies of the Kathmandu Basin Group, central Nepal. *J Nepal Geol Soc* 25. <https://doi.org/10.3126/jngs.v25i0.32043>
- SESAME (2004) Guidelines for the implementation of the H/V spectral ratio technique on ambient vibrations: measurements, processing, and interpretation. European Commission – Research General Directorate.
- Shrestha R, Karanjit S (2017) Comparative study on the fundamental time period of RC buildings based on codal provision and ambient vibration test – a case study of Kathmandu valley. *Journal of Science and Engineering* 4
- Shrestha OM, Koirala A, Hanisch J et al (1999) A geo-environmental map for the sustainable development of the Kathmandu Valley, Nepal. *GeoJournal* 49. <https://doi.org/10.1023/A:1007076813975>
- Shrestha SR, Karkee MB, Cuadra CH et al (2004) Preliminary study for evaluation of earthquake risk to the historical structures in Kathmandu Valley (Nepal). In the proceedings of 13th World Conference on Earthquake Engineering, Vancouver, Canada, p 172
- Stanko D, Markušić S, Strelec S, Gazdek M (2017) HVSR analysis of seismic site effects and soil-structure resonance in Varaždin city (North Croatia). *Soil Dyn Earthq Eng* 92:666–677. <https://doi.org/10.1016/j.soildyn.2016.10.022>
- Takai N, Shigefuji M, Rajaure S et al (2016) Strong ground motion in the Kathmandu Valley during the 2015 Gorkha, Nepal, earthquake 4. *Seismology. Earth Planets Space* 68. <https://doi.org/10.1186/s40623-016-0383-7>
- Tallett-Williams S, Gosh B, Wilkinson S et al (2016) Site amplification in the Kathmandu Valley during the 2015 M7.6 Gorkha Nepal earthquake. *Bull Earthquake Eng* 14:3301–3315. <https://doi.org/10.1007/s10518-016-0003-8>
- Tento A, De Franco R, Franceschina G, Pagani M (2001) Site effect zonation of the Fabriano municipality. *Ital Geotech J* 35(2):131–145
- Thapa DB (1985) Geology and foundation treatment of Kulekhani Dam. Central Nepal, Nepal Journal online
- Towhata I (2007) Developments of soil improvement technologies for mitigation of liquefaction risk. In: *Earthquake Geotechnical Engineering: 4th International Conference on Earthquake Geotechnical Engineering-Invited Lectures*. Springer, pp 355–383
- Yamada M, Hayashida T, Mori J, Mooney WD (2016) Building damage survey and microtremor measurements for the source region of the 2015 Gorkha, Nepal, earthquake. *Earth Planets Space* 68. <https://doi.org/10.1186/s40623-016-0483-4>

Publisher's Note Springer Nature remains neutral with regard to jurisdictional claims in published maps and institutional affiliations.

Springer Nature or its licensor (e.g. a society or other partner) holds exclusive rights to this article under a publishing agreement with the author(s) or other rightsholder(s); author self-archiving of the accepted manuscript version of this article is solely governed by the terms of such publishing agreement and applicable law.